PHYSICAL REVIEW D **88,** 093002 (2013)

Pion form factor and reactions $e^+e^- \to \omega\pi^0$ and $e^+e^- \to \pi^+\pi^-\pi^+\pi^-$ at energies up to 2–3 GeV in the many-channel approach

N. N. Achasov*

Laboratory of Theoretical Physics, S. L. Sobolev Institute for Mathematics, 630090 Novosibirsk, Russian Federation

A. A. Kozhevnikov†

Laboratory of Theoretical Physics, S. L. Sobolev Institute for Mathematics, and Novosibirsk State University, 630090 Novosibirsk, Russian Federation

(Received 28 May 2013; published 7 November 2013)

Using the field-theory-inspired expression for the pion electromagnetic form factor F_π, a good description of the data in the range $-10 < s < 1$ GeV^2 is obtained upon taking into account the pseudoscalar-pseudoscalar (PP) loops. When the vector-pseudoscalar (VP) and the axial vector–pseudoscalar (AP) loops are taken into account in addition to the PP ones, a good description of the *BABAR* data on the reaction $e^+e^- \to \pi^+\pi^-$ is obtained at energies up to 3 GeV. The inclusion of the VP and AP loops demands the treatment of the reactions $e^+e^- \to \omega\pi^0$ and $e^+e^- \to \pi^+\pi^-\pi^+\pi^-$. This task is performed with the SND data on $\omega\pi^0$ production and the *BABAR* data on $\pi^+\pi^-\pi^+\pi^-$ production, both in e^+e^- annihilation, by taking into account $\rho(770)$ and the heavier $\rho(1450)$, $\rho(1700)$, and $\rho(2100)$ resonances. The problems arising from including the VP and AP loops are pointed out and discussed.

DOI: 10.1103/PhysRevD.88.093002 PACS numbers: 13.40.Gp, 12.40.Vv, 13.66.Bc, 14.40.Be

I. INTRODUCTION

Some time ago we suggested a new expression for the electromagnetic form factor of the pion F_π [1–3], which describes the data on the reaction $e^+e^- \to \pi^+\pi^-$ [4–7] restricted to the time-like region $4m_\pi^2 < s \le 1$ GeV^2. The expression takes into account the strong resonance mixing via common decay modes and the $\rho\omega$ mixing. It has both the correct analytical properties and the normalization condition $F_\pi(0) = 1$, and can be represented in the form

$$F_\pi(s) = \frac{1}{\Delta}(g_{\gamma\rho_1}, g_{\gamma\rho_2}, g_{\gamma\rho_3}, \ldots) \times \begin{pmatrix} g_{11} & g_{12} & g_{13} & \cdots & \frac{g_{11}\Pi_{\rho_1\omega}}{D_\omega} \\ g_{12} & g_{22} & g_{23} & \cdots & \frac{g_{12}\Pi_{\rho_1\omega}}{D_\omega} \\ g_{13} & g_{23} & g_{33} & \cdots & \frac{g_{13}\Pi_{\rho_1\omega}}{D_\omega} \\ \cdots & \cdots & \cdots & \cdots & \cdots \\ \frac{g_{11}\Pi_{\rho_1\omega}}{D_\omega} & \frac{g_{12}\Pi_{\rho_1\omega}}{D_\omega} & \frac{g_{13}\Pi_{\rho_1\omega}}{D_\omega} & \cdots & \frac{\Delta}{D_\omega} \end{pmatrix} \times \begin{pmatrix} g_{\rho_1\pi\pi} \\ g_{\rho_2\pi\pi} \\ g_{\rho_3\pi\pi} \\ \cdots \\ 0 \end{pmatrix}, \tag{1.1}$$

where i ($i = 1, 2, 3, \ldots$) counts the ρ-like resonance states $\rho_1 \equiv \rho(770)$, $\rho_2 \equiv \rho(1450)$, $\rho_3 \equiv \rho(1700), \ldots$, and the quantity

$$g_{\gamma V} = \frac{m_V^2}{g_V} \tag{1.2}$$

($V = \rho_{1,2,3,\ldots}, \omega$) is introduced in such a way that $eg_{\gamma V}$ is the γV transition amplitude, where e is the electric charge. As usual, the coupling constant g_V is calculated from the electronic width

$$\Gamma_{V\to e^+e^-} = \frac{4\pi\alpha^2 m_V}{3g_V^2} \tag{1.3}$$

of the resonance V. The quantities g_{ij}/Δ are the matrix elements of the matrix G^{-1} given by Eq. (3.7) below, and $\Delta = \det G$. Ellipses mean additional states, like $\rho(2100)$, etc. It is assumed that the direct G-parity-violating decay $\omega \to \pi^+\pi^-$ is absent, that is, $g_{\omega\pi\pi} = 0$. The quantity $\Pi_{\rho_1\omega}$ is responsible for the $\rho\omega$ mixing. See Ref. [1] for more details concerning Eq. (1.1). We note that an expression similar to Eq. (1.1) was used earlier [8] for the description of data in the time-like domain, but it had a disadvantage in that the normalization condition $F_\pi(0) = 1$ was satisfied only within an accuracy of 20%.

Using the resonance parameters found from fitting the data [4–7], the continuation to the space-like region $s < 0$ was made, and the curve describing the behavior of $F_\pi(s)$ in the range -0.2 GeV$^2 < s < 0$ GeV^2 was obtained [1] and compared with the data [9] in this interval of the momentum transfer squared. The space-like interval was further expanded to $s = -10$ GeV^2 in a subsequent work [3], and a comparison was made with the data [10–12] existing in that interval. The basic ingredient in the above treatment is the inclusion of the pseudoscalar-pseudoscalar (PP) loops, specifically the $\pi^+\pi^-$ and $K\bar{K}$ ones. These contributions are dominant at the center-of-mass energy

*achasov@math.nsc.ru
†kozhev@math.nsc.ru

$\sqrt{s} \leq 1$ GeV. Going to higher energies (up to 3 GeV) of the reaction $e^+e^- \to \pi^+\pi^-$ [7] requires the inclusion of the vector-pseudoscalar (VP) and axial vector–pseudoscalar (AP) intermediate states. This is the aim of the present work. The particular VP state $\omega\pi^0$ produced in e^+e^- annihilation was studied by the SND team in Ref. [13], while the AP state of the type $a_1\pi$ is the intermediate state in the reaction $e^+e^- \to \pi^+\pi^-\pi^+\pi^-$ studied by *BABAR* [14]. An attempt to describe these reactions in the framework of the three-channel approach, taking into account the PP, VP, and AP intermediate states, is also undertaken in the present work. Furthermore, a suitable scheme with three subtractions for the nondiagonal polarization operators is used in the present work, as opposed to Refs. [1–3] where a scheme with two subtractions was used.

Of course, there are many works in the current literature devoted to analyzing the pion form factor in models that are different from that proposed here and in Refs. [1–3]. In particular, a model with a broken hidden local symmetry added to the $\pi^+\pi^-$ and $K\bar{K}$ loops at energies $\sqrt{s} \leq 1$ GeV was used in Refs. [15–17], without attempting to extend the analysis to higher energies. A subtraction scheme different from ours was used there for the calculation of the pseudoscalar-loop contribution. The task of extending the energy region above 1 GeV was undertaken in Ref. [18], taking into account the contributions of heavier rho-like resonances. However, the mixing among these resonances—necessarily arising due to their common decay modes—was not taken into account in that work. A model similar to the K-matrix approach but with improved analytical properties was proposed in Ref. [19]. As opposed to the above works, the present work uses the field-theory-inspired approach to the problem which takes into account relevant PP-, VP-, and AP-loop contributions and the strong mixing of the ρ-like resonances arising via their common decay modes.

The paper is organized as follows. The polarization operators arising due to the (diagonal and nondiagonal) vector-pseudoscalar and axial vector–pseudoscalar loops and the nondiagonal pseudoscalar-pseudoscalar polarization operator are calculated in Sec. II. The expression for the pseudoscalar-pseudoscalar diagonal polarization operator [1–3] is reviewed in the same section. The quantities for comparison with experimental data are discussed in Sec. III. The results of the data fitting are represented in Sec. IV. This section also contains a discussion of the problems that arise when including the VP and AP loops. Section V contains the conclusions drawn from the present study.

II. POLARIZATION OPERATORS DUE TO PSEUDOSCALAR-PSEUDOSCALAR, VECTOR-PSEUDOSCALAR, AND AXIAL VECTOR–PSEUDOSCALAR LOOPS

The final states $\pi^+\pi^-$, $\omega\pi^0$, and $\pi^+\pi^-\pi^+\pi^-$ considered in the present work have the isotopic spin $I = 1$. Hence, they are produced in e^+e^- annihilation via the unit spin ρ-like intermediate states $\rho_1 \equiv \rho(770)$, $\rho_2 \equiv \rho(1450)$, $\rho_3 \equiv \rho(1700)$, etc. These states have rather large widths and are mixed via their common decay modes. The finite-width and mixing effects are taken into account by means of the diagonal and nondiagonal polarization operators $\Pi_{\rho_i\rho_j}$ [1]. In particular, the effects of finite width appear in the inverse propagator of the resonance ρ_i via the replacement

$$m_{\rho_i}^2 - s \to m_{\rho_i}^2 - s - \Pi_{\rho_i\rho_i} \equiv D_i. \tag{2.1}$$

Indeed, according to the unitarity relation, the particular contribution to the imaginary part of the diagonal polarization operator is due to the real intermediate state ab,

$$\begin{aligned} \frac{\Pi_{\rho_i\rho_i}^{(ab)}(s)}{s} &= \frac{1}{\pi}\int_{(m_a+m_b)^2}^{\infty} \frac{\sqrt{s'}\Gamma_{\rho_i\to ab}(s')}{s'(s'-s-i\varepsilon)}\,ds', \\ \mathrm{Im}\Pi_{\rho_i\rho_i}^{(ab)}(s) &= \sqrt{s}\Gamma_{\rho_i\to ab}(s). \end{aligned} \tag{2.2}$$

Hereafter, the quantity s is the energy squared. As explained earlier [1], the dispersion relation written for the polarization operator divided by s automatically guarantees the correct normalization of the form factor $F_\pi(0) = 1$. In the present work, the states which are taken into account are the PP states $\pi^+\pi^-$, $K^+K^- + K^0\bar{K}^0$ of the pair of pseudoscalar mesons, the VP states $\omega\pi^0$, $K^{*+}K^- + K^{*0}\bar{K}^0 + K^{*-}K^+ + \bar{K}^{*0}K^0$, and the AP states $a_1^+(1260)\pi^- + a_1^-(1260)\pi^+$, $K_1(1270)\bar{K}$ + c.c. The polarization operators due to the PP loops are considered in detail elsewhere [1].

The following subtraction scheme is used in the present work. The diagonal polarization operators $\Pi_{\rho_i\rho_i}(s)$ are regularized by making two subtractions: at $s = 0$ and at the respective mass squared $s = m_{\rho_i}^2$, $i = 1, 2, \ldots,$

$$\mathrm{Re}\Pi_{\rho_i\rho_i}(0) = \mathrm{Re}\Pi_{\rho_i\rho_i}(m_{\rho_i}^2) = 0. \tag{2.3}$$

The nondiagonal polarization operators $\Pi_{\rho_i\rho_j}(s)$, $i \neq j$, are regularized by making three subtractions: at $s = 0$, at $s = m_{\rho_i}^2$, and at $s = m_{\rho_j}^2$ $i, j = 1, 2, \ldots,$

$$\mathrm{Re}\Pi_{\rho_i\rho_j}(0) = \mathrm{Re}\Pi_{\rho_i\rho_j}(m_{\rho_i}^2) = \mathrm{Re}\Pi_{\rho_i\rho_j}(m_{\rho_j}^2) = 0. \tag{2.4}$$

The corresponding expression, in the case of the two-particle state ab, is

$$\Pi_{\rho_i\rho_j}^{(ab)}(s) = g_{\rho_i ab}g_{\rho_j ab}\Pi_{\rho_i\rho_j}(s, m_{\rho_i}, m_{\rho_j}, m_a, m_b), \tag{2.5}$$

where

$$\Pi_{\rho_i\rho_j}(s, m_{\rho_i}, m_{\rho_j}, m_a, m_b) = \frac{s}{m^2_{\rho_i} - m^2_{\rho_j}}\left[\frac{\mathrm{Re}G^{(ab)}(m^2_{\rho_i})}{m^2_{\rho_i}}(m^2_{\rho_j} - s) - \frac{\mathrm{Re}G^{(ab)}(m^2_{\rho_j})}{m^2_{\rho_j}}(m^2_{\rho_i} - s)\right] + G^{(ab)}(s), \quad (2.6)$$

while $G^{(ab)}(s) \equiv G^{(ab)}(s, m_a, m_b)$,

$$G^{(ab)}(s, m_a, m_b) = \frac{s^3}{\pi g^2_{\rho_i ab}}\int_{(m_a+m_b)^2}^{\infty}\frac{\sqrt{s'}\Gamma_{\rho_i ab}(s')ds'}{s'^3(s' - s - i0)}, \quad (2.7)$$

with $g_{\rho_i ab}$ and $\Gamma_{\rho_i ab}$ being the coupling constant and the partial width of the decay $\rho_i \to ab$, respectively. The specific expressions for $G^{(ab)}$ and other necessary quantities are given below. Note that a different scheme with two subtractions for the nondiagonal PP polarization operators was used in Ref. [1–3].

A. Pseudoscalar-pseudoscalar loop

The diagonal polarization operators due to the PP loop are represented in the form

$$\Pi^{(\mathrm{PP})}_{\rho_i\rho_i} = g^2_{\rho_i \mathrm{PP}}\Pi^{(\mathrm{PP})}. \quad (2.8)$$

The function $\Pi^{(\mathrm{PP})}$ is

$$\Pi^{(\mathrm{PP})} \equiv \Pi^{(\mathrm{PP})}(s, m_V, m_P) = \Pi^{(\mathrm{PP})}_0 + \Pi^{(\mathrm{PP})}_1, \quad (2.9)$$

where

$$\Pi^{(\mathrm{PP})}_0 = \frac{s}{48\pi^2}\left[8m^2_P\left(\frac{1}{m^2_V} - \frac{1}{s}\right) + v^3_P(m^2_V)\ln\frac{1 + v_P(m^2_V)}{1 + v_P(m^2_V)}\theta(m_V - 2m_P) - 2\bar{v}^3_P(m^2_V)\arctan\frac{1}{\bar{v}_P}\theta(2m_P - m_V)\right],$$

$$\Pi^{(\mathrm{PP})}_1 = \frac{s}{48\pi^2}\left\{\theta(s - 4m^2_P)v^3_P(s)\left[i\pi - \ln\frac{1 + v_P(s)}{1 - v_P(s)}\right] + 2\theta(4m^2_P - s)\theta(s)\bar{v}^3_P(s)\arctan\frac{1}{\bar{v}_P(s)} - \theta(-s)v^3_P(s)\ln\frac{v_P(s) + 1}{v_P(s) - 1}\right\}, \quad (2.10)$$

and [20]

$$v_P(s) = \sqrt{1 - \frac{4m^2_P}{s}}, \qquad \bar{v}_P(s) = \sqrt{\frac{4m^2_P}{s} - 1},$$

where θ is the step function.

The function $G^{(\mathrm{PP})}(s)$ [Eq. (2.7)] necessary for the evaluation of the nondiagonal polarization operator due to the PP loop is

$$G^{(\mathrm{PP})}(s) = \frac{1}{24\pi^2}\left\{\frac{s}{4m^2_P}\left[\frac{2}{15} + \frac{2}{3}v^2_P(s) - v^4_P(s)\right] - \frac{1}{2}\theta(-s)v^3_P(s)\ln\frac{v_P(s) + 1}{v_P(s) - 1} + \theta(4m^2_P - s)\theta(s)\bar{v}_P(s)\arctan\frac{1}{\bar{v}_P(s)} + \frac{1}{2}\theta(s - 4m^2_P)v^3_P(s)\left[i\pi - \ln\frac{1 + v_P(s)}{1 - v_P(s)}\right]\right\}. \quad (2.11)$$

B. Vector-pseudoscalar loop

The diagonal polarization operators due to the VP loop are represented in the form

$$\Pi^{(\mathrm{VP})}_{\rho_i\rho_i} = g^2_{\rho_i \mathrm{VP}}\Pi^{(\mathrm{VP})}, \quad (2.12)$$

where the function $\Pi^{(\mathrm{VP})} \equiv \Pi^{(\mathrm{VP})}(s, m_{\rho_i}, m_V, m_P)$ is calculated from the dispersion relation

$$\frac{\Pi^{(\mathrm{VP})}}{s} = \frac{1}{12\pi^2}\int_{(m_V+m_P)^2}^{\infty}\frac{q^3_{\mathrm{VP}}(s', m_V, m_P)}{\sqrt{s'}(s' - s - i\varepsilon)}\left(\frac{s_0 + m^2_{\rho_i}}{s_0 + s'}\right)ds'. \quad (2.13)$$

The notations are as follows. The quantity

$$q_{ab}(s, m_a, m_b) = [s^2 - 2(m^2_a + m^2_b) + (m^2_a - m^2_b)^2]^{1/2}/2\sqrt{s} \quad (2.14)$$

is the momentum of the particle a or b in the rest frame of the decaying particle with the invariant mass $\sqrt{s}$; m_{ρ_i}, m_V, and m_P are, respectively, the masses of the resonance ρ_i, and the vector V and pseudoscalar P mesons propagating in the loop, and $g_{\rho_i \mathrm{VP}}$ is the coupling constant of the resonance ρ_i with the VP state. It is well known that the partial width of the decay $\rho_i \to VP$,

$$\Gamma_{\rho_i \mathrm{VP}}(s) = \frac{g^2_{\rho_i \mathrm{VP}}}{12\pi}q^3_{\mathrm{VP}}(s, m_V, m_P),$$

grows as the energy increases. This growth spoils the convergence of the integral (2.13). This is the reason for the appearance of the function $(s_0 + m^2_{\rho_i})/(s' + m^2_{\rho_i})$ in the integrand of Eq. (2.13). It suppresses the fast growth of the partial width and improves the convergence of the above integral at large s'. However, the integral still remains logarithmically divergent, and one should perform the subtraction of the real part $\mathrm{Re}\Pi^{(\mathrm{VP})}_{\rho_i\rho_i}/s$ at $s = m^2_{\rho_i}$.

The expression for $\Pi^{(\mathrm{VP})}$ resulting from Eq. (2.13) can be represented in the form

$$\Pi^{(\mathrm{VP})} = \frac{1}{96\pi^2}[\Pi^{(\mathrm{VP})}_0 + \Pi^{(\mathrm{VP})}_1 + \Pi^{(\mathrm{VP})}_2], \quad (2.15)$$

where

$$\Pi_0^{(\mathrm{VP})} = \frac{m_{\rho_i}^2 + s_0}{s_0^2}\left(1 - \frac{s}{m_{\rho_i}^2}\right)\left\{(m_+m_-)^3\left[1 - \frac{s_0}{s}\left(1 + \frac{s}{m_{\rho_i}^2}\right)\right]\ln\frac{m_V}{m_P} + m_+m_-\left[\frac{3}{2}(m_+^2 + m_-^2)\ln\frac{m_V}{m_P} + m_+m_-\right]s_0\right.$$
$$\left. - \frac{sm_{\rho_i}^2}{(s+s_0)(m_{\rho_i}^2+s_0)}[(m_+^2+s_0)(m_-^2+s_0)]^{3/2}\ln\frac{\sqrt{m_+^2+s_0}+\sqrt{m_-^2+s_0}}{\sqrt{m_+^2+s_0}-\sqrt{m_-^2+s_0}}\right\},$$

$$\Pi_1^{(\mathrm{VP})} = -\frac{s}{m_{\rho_i}^4}|(m_+^2 - m_{\rho_i}^2)(m_{\rho_i}^2 - m_-^2)|^{3/2}\left[2\theta(m_+ - m_{\rho_i})\theta(m_{\rho_i} - m_-)\arctan\sqrt{\frac{m_{\rho_i}^2 - m_-^2}{m_+^2 - m_{\rho_i}^2}} - \theta(m_{\rho_i} - m_+)\right.$$
$$\left.\times\ln\frac{\sqrt{m_{\rho_i}^2 - m_-^2}+\sqrt{m_{\rho_i}^2 - m_+^2}}{\sqrt{m_{\rho_i}^2 - m_-^2}-\sqrt{m_{\rho_i}^2 - m_+^2}} + \theta(m_- - m_{\rho_i})\ln\frac{\sqrt{m_+^2 - m_{\rho_i}^2}+\sqrt{m_-^2 - m_{\rho_i}^2}}{\sqrt{m_+^2 - m_{\rho_i}^2}-\sqrt{m_-^2 - m_{\rho_i}^2}}\right],$$

$$\Pi_2^{(\mathrm{VP})} = \frac{m_{\rho_i}^2 + s_0}{s(s+s_0)}|(m_+^2 - s)(m_-^2 - s)|^{3/2}\left[\theta(m_-^2 - s)\ln\frac{\sqrt{m_+^2 - s}+\sqrt{m_-^2 - s}}{\sqrt{m_+^2 - s}-\sqrt{m_-^2 - s}} + 2\theta(s - m_-^2)\theta(m_+^2 - s)\arctan\sqrt{\frac{s - m_-^2}{m_+^2 - s}}\right.$$
$$\left. + \theta(s - m_+^2)\left(i\pi - \ln\frac{\sqrt{s - m_-^2}+\sqrt{s - m_+^2}}{\sqrt{s - m_-^2}-\sqrt{s - m_+^2}}\right)\right], \tag{2.16}$$

while $m_\pm = m_V \pm m_P$, and θ is the usual step function. The dependence of $\mathrm{Re}\Pi_{\rho_1\rho_1}^{(\mathrm{VP})}(s)$ on the energy squared at $s_0 = 0.09\ \mathrm{GeV}^2$ is shown in Fig. 1.

The function $G^{(\mathrm{VP})}(s)$ [Eq. (2.7)] necessary for the evaluation of the nondiagonal polarization operator due to the VP loop is

$$G^{(\mathrm{VP})}(s) = \frac{s^2}{48\pi^2}\left(\frac{4m_Vm_P}{m_+m_-}\right)^3 I^{(\mathrm{VP})}(s), \tag{2.17}$$

where

$$I^{(\mathrm{VP})}(s) = \left\{\frac{s^3}{16} + \frac{m_+^2}{4m_Vm_P}(s - m_-^2)\left[\frac{3s^2}{8} - \frac{m_+^2 s(s - m_-^2)}{8m_Vm_P} - \left(\frac{m_+m_-}{4m_Vm_P}\right)^2(m_+^2 - s)(s - m_-^2)\right]\right\}\frac{1}{2s^3}\ln\frac{m_V}{m_P}$$
$$+ \frac{m_+m_-}{4m_Vm_Ps^3}\left\{\frac{s^2m_-^2}{4m_Vm_P}\left[\frac{s}{24} + \frac{m_+^2(s - m_-^2)}{16m_Vm_P} + \frac{sm_-^2}{24m_Vm_P}\right] - \frac{s^3}{16} - \frac{sm_+^2(s - m_-^2)}{4m_Vm_P}\left[\frac{3s}{8} - \frac{m_+^2(s - m_-^2)}{8m_Vm_P}\right]\right\}$$
$$+ \left(\frac{m_+m_-}{4m_Vm_Ps}\right)^3|(s - m_+^2)(s - m_-^2|^{3/2}\times\left[\frac{1}{2}\theta(m_-^2 - s)\ln\frac{\sqrt{m_+^2 - s}+\sqrt{m_-^2 - s}}{\sqrt{m_+^2 - s}-\sqrt{m_-^2 - s}}\right.$$
$$\left. + \theta(s - m_-^2)\theta(m_+^2 - s)\arctan\sqrt{\frac{s - m_-^2}{m_+^2 - s}} + \frac{1}{2}\theta(s - m_+^2)\left(i\pi - \ln\frac{\sqrt{s - m_-^2}+\sqrt{s - m_+^2}}{\sqrt{s - m_-^2}-\sqrt{s - m_+^2}}\right)\right]. \tag{2.18}$$

The dependence of $\mathrm{Re}\Pi_{\rho_1\rho_2}^{(\omega\pi)}/g_{\omega\rho_1\pi}g_{\omega\rho_2\pi}$ on s is shown in Fig. 2.

C. Axial vector–pseudoscalar loop

The axial vector–pseudoscalar meson state $\mathrm{AP} = a_1(1260)\pi$ is considered to be one of the states contributing to the four-pion production amplitude [21]. For soft pions, when taking into account the requirements of chiral symmetry, this amplitude and the corresponding partial width are very complicated [22–28]. This prevents one from using the dispersion relation to obtain the contribution of the four-pion state to the polarization operator of the state ρ_i. Hence, in the present work, the simplest $a_1\pi$ dominance model of the four-pion [29] production is used: $e^+e^- \to \rho_i \to a_1\pi \to 4\pi$. The amplitude of the transition $\rho_i \to a_1\pi$ is chosen in the simplest form,

$$A(\rho_{iq} \to a_{1k}\pi_p) = g_{\rho_i a_1\pi}[(\epsilon_{a_1}\epsilon_{\rho_i})(kq) - (\epsilon_{a_1}q)(\epsilon_{\rho_i}k)], \tag{2.19}$$

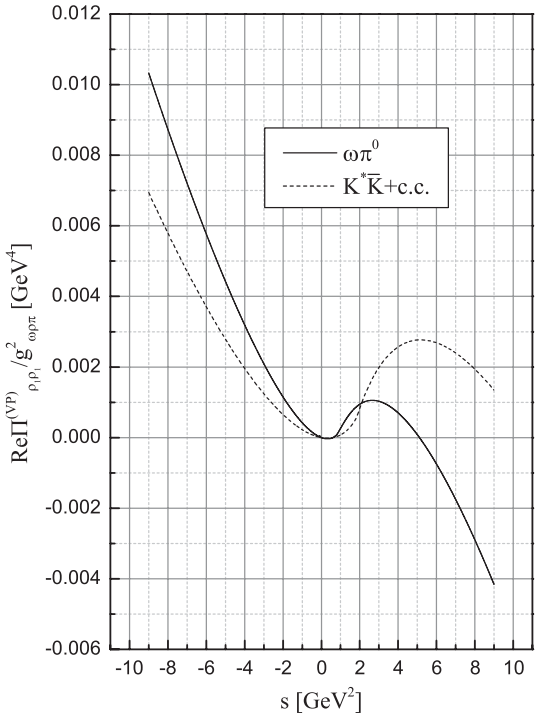

FIG. 1. The dependence of $\mathrm{Re}\Pi^{(\mathrm{VP})}_{\rho_1\rho_1}(s)/g^2_{\omega\rho_1\pi}$ on the energy squared; $s_0 = 0.09$ GeV^2.

where q, k, and p are, respectively, the four-momenta of the mesons ρ_i, a_1, and π, while ϵ_{a_1} and ϵ_{ρ_i} denote the polarization four-vectors of a_1 and ρ_i. The expression (2.19) is chosen on the grounds that it is explicitly transverse in the ρ_i leg.

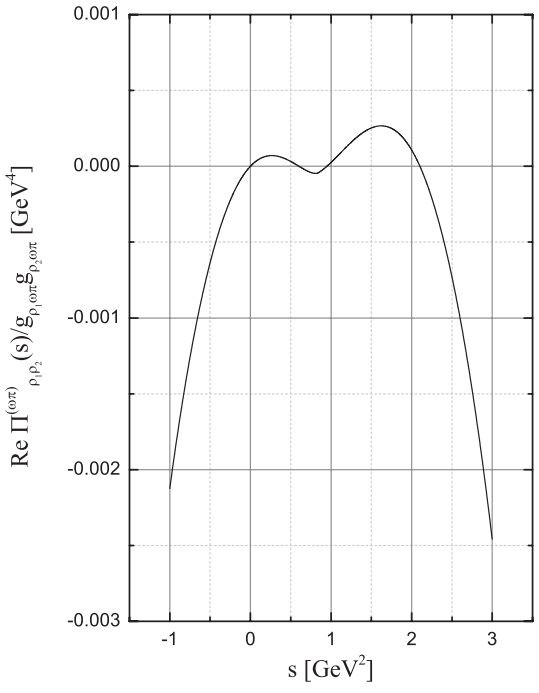

FIG. 2. The dependence of $\mathrm{Re}\Pi^{(\omega\pi)}_{\rho_1\rho_2}(s)/g_{\omega\rho_1\pi}g_{\omega\rho_2\pi}$ on the energy squared in the case of $m_{\rho_1} = 770$ MeV and $m_{\rho_2} = 1450$ MeV.

The diagonal polarization operators due to the AP loop are represented in the form

$$\Pi^{(\mathrm{AP})}_{\rho_i\rho_i} = g^2_{\rho_i\mathrm{AP}}\Pi^{(\mathrm{AP})}, \tag{2.20}$$

where the quantity $\Pi^{(\mathrm{AP})} \equiv \Pi^{(\mathrm{AP})}(s, m_{\rho_i}, m_A, m_P)$ is calculated from the dispersion relation

$$\frac{\Pi^{(\mathrm{AP})}}{s} = \frac{1}{48\pi^2}\int_{(m_A+m_P)^2}^{\infty}\frac{q_{\mathrm{AP}}(s', m_A, m_P)}{(s')^{3/2}(s' - s - i\varepsilon)} \times [(s' + m_A^2 - m_P^2)^2 + 2s'm_A^2] \times \left(\frac{s_0 + m^2_{\rho_i}}{s_0 + s'}\right)ds', \tag{2.21}$$

where the expression

$$\Gamma_{\rho_i\to\mathrm{AP}}(s) = \frac{g^2_{\rho_i\mathrm{AP}}}{48\pi s}[(s + m_A^2 - m_P^2)^2 + 2sm_A^2] \times q_{\mathrm{AP}}(s, m_A, m_P)\left(\frac{s_0 + m^2_{\rho_i}}{s_0 + s}\right) \tag{2.22}$$

for the $\rho_i \to \mathrm{AP}$ decay width found from the effective vertex (2.19) is inserted into the integrand of the dispersion relation. The result of integration is represented in the form

$$\Pi^{(\mathrm{AP})} = \frac{s}{96\pi^2}\left(\frac{m_-}{m_+}\right)^3\frac{m^2_{\rho_i} + s_0}{s + s_0}\left[J(s) - \mathrm{Re}J(m^2_{\rho_i})\frac{s + s_0}{m^2_{\rho_i} + s_0}\right], \tag{2.23}$$

where $m_\pm = m_A \pm m_P$, and

$$J(s) = sf(s)\left[\left(\frac{m_+^2}{s} - 1\right)^2 + \frac{2m_A}{m_-}\left(2 + \frac{m_A}{m_-}\right)\left(\frac{m_+^2}{s} - 1\right) + 6\frac{m_A^2}{m_-^2}\right] - s_0 f_2\left[\left(\frac{m_+^2}{s_0} + 1\right)^2 - \frac{2m_A}{m_-}\left(2 + \frac{m_A}{m_-}\right)\left(\frac{m_+^2}{s_0} + 1\right) + 6\frac{m_A^2}{m_-^2}\right]. \tag{2.24}$$

The function $f(s)$ is

$$f(s) = \frac{m_+}{sm_-}\left\{(s - m_-^2)\frac{m_+}{m_-}\ln\frac{m_A}{m_P} - s\left(\frac{m_+^2 - m_-^2}{2m_+m_-}\ln\frac{m_A}{m_P} - 1\right) + \sqrt{|(s - m_+^2)(s - m_-^2)|} \times \left[\theta(m_-^2 - s)\ln\frac{\sqrt{m_+^2 - s} + \sqrt{m_-^2 - s}}{\sqrt{m_+^2 - s} + \sqrt{m_-^2 - s}} - 2\theta(s - m_-^2)\theta(m_+^2 - s)\arctan\sqrt{\frac{s - m_-^2}{m_+^2 - s}} - \theta(s - m_+^2)\left(-i\pi + \ln\frac{\sqrt{s - m_-^2} + \sqrt{s - m_+^2}}{\sqrt{s - m_-^2} - \sqrt{s - m_+^2}}\right)\right]\right\}, \tag{2.25}$$

and

$$f_2 = -\frac{m_+}{m_-}\left[\frac{m_+}{m_-}\left(1+\frac{m_-^2}{s_0}\right)\left(\ln\frac{m_A}{m_P} - \frac{2m_-}{m_+}\sqrt{\frac{m_+^2+s_0}{m_-^2+s_0}}\right.\right.$$
$$\left.\left.\times \tanh^{-1}\sqrt{\frac{m_-^2+s_0}{m_+^2+s_0}}\right) - \frac{m_+^2-m_-^2}{2m_+m_-}\ln\frac{m_A}{m_P} + 1\right]. \quad (2.26)$$

The dependence of $\mathrm{Re}\Pi^{(\mathrm{AP})}_{\rho_1\rho_1}(s)$ on the energy squared is shown in Fig. 3.

The function $G^{(\mathrm{AP})}(s)$ [Eq. (2.7)] necessary for the evaluation of the nondiagonal polarization operator due to the AP loop is

$$G^{(\mathrm{AP})}(s) = \frac{s^2}{48\pi^2}\left(\frac{4m_Am_P}{m_+m_-}\right)^3 I^{(\mathrm{AP})}(s), \quad (2.27)$$

where

$$I^{(\mathrm{AP})}(s) = \left\{\frac{1}{16} + \frac{m_-^2}{32m_Am_P}\left(\frac{m_+^2}{s}-1\right) + \frac{m_A+2m_-}{16m_P} + \frac{1}{2}\left(\frac{m_+m_-}{4m_Am_P}\right)^2\left(\frac{m_+^2}{s}-1\right)\left(1-\frac{m_-^2}{s}\right) - \frac{m_-^2(m_A+2m_P)}{16m_Am_P^2} - \frac{3m_-^2}{16m_P^2}\right.$$
$$+\frac{m_+^2}{4m_Am_P}\left(1-\frac{m_-^2}{s}\right)\left[\left(\frac{m_-^2}{4m_Am_P}\right)^2\left(\frac{m_+^2}{s}-1\right)^2 + \frac{m_-^2}{2m_Am_P}\left(\frac{m_+^2}{s}-1\right) + \frac{3m_-^2}{8m_P^2}\right]\Bigg\} \times \frac{1}{2}\ln\frac{m_A}{m_P} + \frac{m_+m_-}{4m_Am_P}\left\{\frac{1}{6}\left(\frac{m_+^2}{4m_Am_P}\right)^2\right.$$
$$+\frac{m_-^2}{4m_Am_P}\left[\frac{1}{24} - \frac{m_-^2}{16m_Am_P}\left(\frac{m_+^2}{s}-1\right) - \frac{m_A+2m_-}{8m_P}\right] - \frac{1}{16} + \frac{3m_-^2}{32m_Am_P}\left(\frac{m_+^2}{s}-1\right) + \frac{3(m_A+2m_-)}{16m_P}$$
$$-\frac{1}{2}\left(\frac{m_+m_-}{4m_Am_P}\right)^2\left(\frac{m_+^2}{s}-1\right)\left(1-\frac{m_-^2}{s}\right) - \frac{m_+^2(m_A+2m_P)}{16m_Am_P^2}\left(1-\frac{m_-^2}{s}\right) + \frac{3m_-^2}{16m_P^2} + \frac{1}{s}\left[\left(\frac{m_-^2}{4m_Am_P}\right)^2\left(\frac{m_+^2}{s}-1\right)^2\right.$$
$$\left.+\frac{m_-^2}{2m_Am_P}\left(\frac{m_+^2}{s}-1\right) + \frac{3m_-^2}{8m_P^2}\right]|(s-m_-^2)(s-m_+^2)|^{1/2}\left[\frac{1}{2}\theta(m_-^2-s)\ln\frac{\sqrt{m_+^2-s}+\sqrt{m_-^2-s}}{\sqrt{m_+^2-s}-\sqrt{m_-^2-s}}\right.$$
$$\left.\left.\left.-\theta(s-m_-^2)\theta(m_+^2-s)\arctan\sqrt{\frac{s-m_-^2}{m_+^2-s}} + \frac{1}{2}\theta(s-m_+^2)\left(i\pi - \ln\frac{\sqrt{s-m_-^2}+\sqrt{s-m_+^2}}{\sqrt{s-m_-^2}-\sqrt{s-m_+^2}}\right)\right]\right\}. \quad (2.28)$$

The dependence of $\mathrm{Re}\Pi^{(a_1\pi)}_{\rho_1\rho_2}/g_{a_1\rho_1\pi}g_{a_1\rho_2\pi}$ on s is shown in Fig. 4.

D. Polarization operators used in fits

Although the nature of the higher resonances $\rho(1450)$, $\rho(1700)$, ... is the subject of current and future studies, the quark-antiquark model relations between their coupling constants are assumed,

$$g_{\rho_iK^*K} = \frac{1}{2}g_{\rho_i\omega\pi}, \quad g_{\rho_iK_1(1270)K} = \frac{1}{2}g_{\rho_ia_1(1260)\pi}. \quad (2.29)$$

Polarization operators which take into account the three channels described above are the following. The full diagonal polarization operators are

$$\Pi_{\rho_i\rho_i} = \Pi^{(\mathrm{PP})}_{\rho_i\rho_i} + \Pi^{(\mathrm{VP})}_{\rho_i\rho_i} + \Pi^{(\mathrm{AP})}_{\rho_i\rho_i}. \quad (2.30)$$

In the present work, we take into account the following analytically calculated loops. First, we use the PP $\pi^+\pi^-$ and $K^+K^- + K^0\bar{K}^0$ loops,

$$\Pi^{(\mathrm{PP})}_{\rho_i\rho_i} = g^2_{\rho_i\pi\pi}\left[\Pi^{(\mathrm{PP})}(s, m_{\rho_i}, m_\pi) + \frac{1}{2}\Pi^{(\mathrm{PP})}(s, m_{\rho_i}, m_K)\right], \quad (2.31)$$

with $\Pi^{(\mathrm{PP})}$ given by Eq. (2.9). Second, we use the VP $\omega\pi^0$ and $K^*\bar{K}^+\bar{K}^*K$ loops,

$$\Pi^{(\mathrm{VP})}_{\rho_i\rho_i} = g^2_{\rho_i\omega\pi}[\Pi^{(\mathrm{VP})}(s, m_{\rho_i}, m_\omega, m_\pi) + \Pi^{(\mathrm{VP})}(s, m_{\rho_i}, m_{K^*}, m_K)], \quad (2.32)$$

with $\Pi^{(\mathrm{VP})} \equiv \Pi^{(\mathrm{VP})}(s, m_{\rho_i}, m_V, m_P)$ given by Eq. (2.15). Third, we use the AP $a_1(1260)^+\pi^- + a_1(1260)^-\pi^+$, $K_1(1270)\bar{K}$ + c.c. loops,

$$\Pi^{(\mathrm{AP})}_{\rho_i\rho_i} = 2g^2_{\rho_ia_1\pi}\left[\Pi^{(\mathrm{AP})}(s, m_{\rho_i}, m_{a_1}, m_\pi) + \frac{1}{2}\Pi^{(\mathrm{AP})}(s, m_{\rho_i}, m_{K_1(1270)}, m_K)\right], \quad (2.33)$$

with $\Pi^{(\mathrm{AP})} \equiv \Pi^{(\mathrm{AP})}(s, m_{\rho_i}, m_A, m_P)$ given by Eq. (2.23).

Similar expressions are used for the nondiagonal polarization operators,

$$\Pi_{\rho_i\rho_j} = \Pi^{(\mathrm{PP})}_{\rho_i\rho_j} + \Pi^{(\mathrm{VP})}_{\rho_i\rho_j} + \Pi^{(\mathrm{AP})}_{\rho_i\rho_j}, \quad (2.34)$$

where

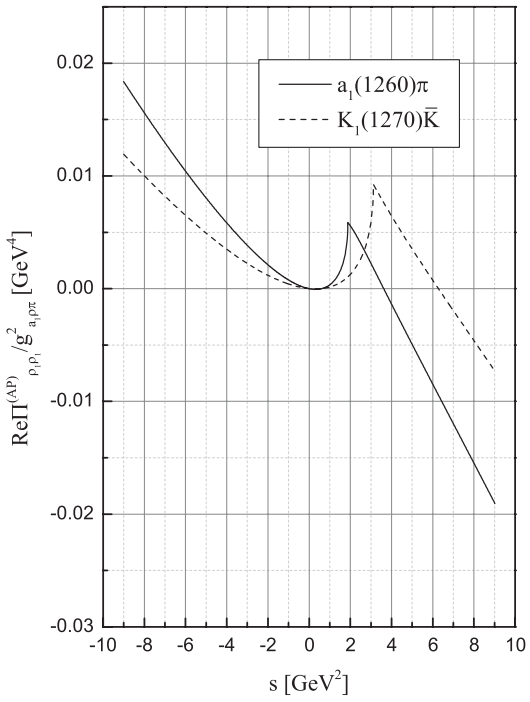

FIG. 3. The dependence of $\mathrm{Re}\Pi^{(\mathrm{AP})}_{\rho_1\rho_1}(s)$ on the energy squared s for the $AP = a_1(1260)\pi$ and $AP = K_1(1270)\bar{K}$ loops, demonstrating the discontinuity of $\frac{d\mathrm{Re}\Pi^{(\mathrm{AP})}}{ds}$ at $s = (m_A + m_P)^2$. The parameters are $m_\rho = 777$ MeV, $m_{a_1} = 1230$ MeV, $m_{K_1} = 1270$ MeV, $s_0 = 0.09$ GeV^2.

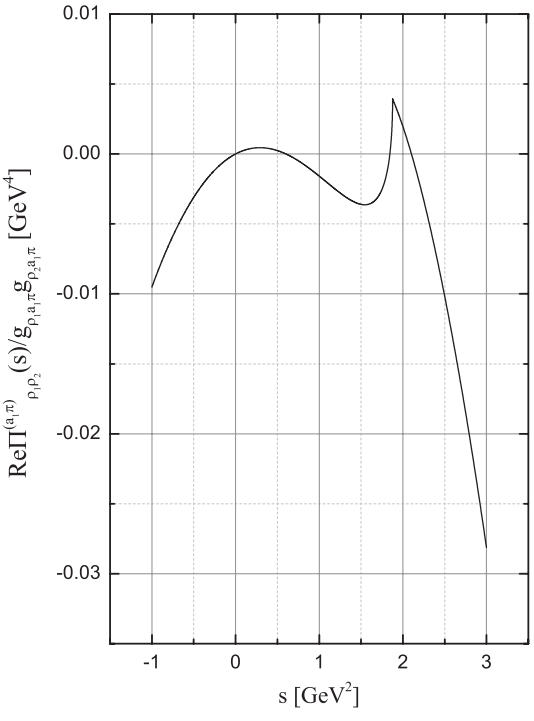

FIG. 4. The dependence of $\mathrm{Re}\Pi^{(a_1\pi)}_{\rho_1\rho_2}(s)/g_{a_1\rho_1\pi}g_{a_1\rho_2\pi}$ on the energy squared in the case of $m_{\rho_1} = 770$ MeV and $m_{\rho_2} = 1450$ MeV.

$$\Pi^{(\mathrm{PP})}_{\rho_i\rho_j} = g_{\rho_i\pi\pi}g_{\rho_j\pi\pi}\Big[\Pi_{\rho_i\rho_j}(s, m_{\rho_i}, m_{\rho_j}, m_\pi, m_\pi) + \frac{1}{2}\Pi_{\rho_i\rho_j}(s, m_{\rho_i}, m_{\rho_j}, m_K, m_K)\Big],$$
$$\Pi^{(\mathrm{VP})}_{\rho_i\rho_j} = g_{\rho_i\omega\pi}g_{\rho_j\omega\pi}[\Pi_{\rho_i\rho_j}(s, m_{\rho_i}, m_{\rho_j}, m_\omega, m_\pi) + \Pi_{\rho_i\rho_j}(s, m_{\rho_i}, m_{\rho_j}, m_{K^*}, m_K)],$$
$$\Pi^{(\mathrm{AP})}_{\rho_i\rho_j} = 2g_{\rho_i a_1\pi}g_{\rho_j a_1\pi}\Big[\Pi_{\rho_i\rho_j}(s, m_{\rho_i}, m_{\rho_j}, m_{a_1}, m_\pi) + \frac{1}{2}\Pi_{\rho_i\rho_j}(s, m_{\rho_i}, m_{\rho_j}, m_{K_1}, m_K)\Big], \quad (2.35)$$

with $\Pi_{\rho_i\rho_j}(s, m_{\rho_i}, m_{\rho_j}, m_a, m_b)$ given by Eq. (2.6), and the corresponding functions $G^{(ab)}(s)$ are given in Eqs. (2.11), (2.17), and (2.27).

III. QUANTITIES FOR COMPARISON WITH THE DATA

The following reactions are considered in the present work:

$$e^+e^- \to \pi^+\pi^-, \quad (3.1)$$

$$e^+e^- \to \omega\pi^0, \quad (3.2)$$

and

$$e^+e^- \to \pi^+\pi^-\pi^+\pi^-. \quad (3.3)$$

The justification of the restriction to these reactions are given in the Introduction and below in Sec. IV. Let us turn to the working expressions necessary for comparison with the experimental data.

A. $\pi^+\pi^-$ production

In the present case, the relevant quantity is the so-called bare cross section of the reaction (3.1),

$$\sigma_{\mathrm{bare}} = \frac{8\pi\alpha^2}{3s^{5/2}}|F_\pi(s)|^2 q^3_\pi(s)\Big[1 + \frac{\alpha}{\pi}a(s)\Big], \quad (3.4)$$

where $F_\pi(s)$ is the pion form factor (1.1), the quantity $a(s)$ takes into account the radiation by the final pions, and $\alpha = 1/137$ is the fine-structure constant. The necessary discussion concerning the quantities in Eq. (3.4) are given elsewhere [1].

B. $\omega\pi^0$ production

The cross section of the reaction $e^+e^- \to \omega\pi^0$ is taken in the form

$$\sigma_{e^+e^-\to\omega\pi^0} = \frac{4\pi\alpha^2}{3s^{3/2}}|A_{e^+e^-\to\omega\pi^0}|^2 \times q^3_{\omega\pi}(s, m_\omega, m_\pi), \quad (3.5)$$

where $q_{\omega\pi}$ is given by Eq. (2.14),

$$A_{e^+e^-\to\omega\pi^0} = (g_{\gamma\rho_1}, g_{\gamma\rho_2}, g_{\gamma\rho_3}, \ldots)G^{-1}\times\begin{pmatrix} g_{\rho_1\omega\pi} \\ g_{\rho_2\omega\pi} \\ g_{\rho_3\omega\pi} \\ \cdots \end{pmatrix} \tag{3.6}$$

is the amplitude of the reaction, and the matrix

$$G = \begin{pmatrix} D_1 & -\Pi_{12} & -\Pi_{13} & \cdots \\ -\Pi_{12} & D_2 & -\Pi_{23} & \cdots \\ -\Pi_{13} & -\Pi_{23} & D_3 & \cdots \\ \cdots & \cdots & \cdots & \end{pmatrix} \tag{3.7}$$

is introduced in order to take into account the strong mixing of the resonances ρ_i [1]. Here, $\Pi_{ij} \equiv \Pi_{\rho_i\rho_j}$ are the polarization operators; see Eqs. (2.30) and (2.34). The nondiagonal $i \neq j$ terms describe the mixing. The inverse propagators D_i are given by Eq. (2.1).

C. $\pi^+\pi^-\pi^+\pi^-$ production

The width of the decay $\rho_i \to 2\pi^+2\pi^-$ in the model (2.19) is represented in the form

$$\Gamma_{\rho_i\to 2\pi^+2\pi^-}(s) = g^2_{\rho_i a_1\pi} W_{\pi^+\pi^-\pi^+\pi^-}(s), \tag{3.8}$$

where

$$W_{\pi^+\pi^-\pi^+\pi^-}(s) = \frac{1}{12\pi}\int_{(3m_\pi)^2}^{(\sqrt{s}-m_\pi)^2} \rho_{a_1}(m^2) \times\left[\frac{(s+m^2-m_\pi^2)^2}{2s}+m^2\right] \times q_{a_1\pi}(s, m^2, m_\pi^2)dm^2, \tag{3.9}$$

and $q_{a_1\pi}$ is given by Eq. (2.14). The function

$$\rho_{a_1}(m^2) = \frac{m_{a_1}\Gamma_{a_1}/\pi}{(m^2-m_{a_1}^2)^2 + m_{a_1}^2\Gamma_{a_1}^2} \tag{3.10}$$

is introduced to take into account the large width of the intermediate a_1 resonance in a minimal way, by taking the limit of the fixed a_1 width. The mass and width of $a_1(1260)$ are determined from fitting the data on the reaction $e^+e^- \to \pi^+\pi^-\pi^+\pi^-$.

The cross section of the reaction $e^+e^- \to \pi^+\pi^-\pi^+\pi^-$ is represented in the form

$$\sigma_{\pi^+\pi^-\pi^+\pi^-} = \frac{(4\pi\alpha)^2}{3s^{3/2}}\left|(g_{\gamma\rho_1}, g_{\gamma\rho_2}, g_{\gamma\rho_3}, \ldots)G^{-1}\begin{pmatrix} g_{\rho_1 a_1\pi} \\ g_{\rho_2 a_1\pi} \\ g_{\rho_3 a_1\pi} \\ \cdots \end{pmatrix}\right|^2 \times W_{\pi^+\pi^-\pi^+\pi^-}(s), \tag{3.11}$$

where $W_{\pi^+\pi^-\pi^+\pi^-}(s)$ [given by Eq. (3.9)] represents the effective phase-space volume of the four pions via the smearing [Eq. (3.10)] of the $a_1\pi$ phase-space volume. The matrix G is the matrix of inverse propagators, Eq. (3.7).

IV. RESULTS OF DATA FITTING

This section is devoted to the presentation of the results of fitting the data on the reactions $e^+e^- \to \pi^+\pi^-$, $e^+e^- \to \omega\pi^0$, and $e^+e^- \to \pi^+\pi^-\pi^+\pi^-$. Two possible fitting schemes were used.

Scheme 1: Three resonances $\rho(770) + \rho(1450) + \rho(1700)$ and the PP loops of pseudoscalar mesons are taken into account [1,2].

When adding the VP- and AP-loop contributions to the pion form factor one should also include the VP and AP final states. These states manifest, respectively, in the reactions $e^+e^- \to \omega\pi^0$ and $e^+e^- \to \pi^+\pi^-\pi^+\pi^-$, which should also be treated in the present framework. Since energies higher than 2 GeV are considered, the third heavy isovector resonance $\rho(2100)$ is added. Hence, the scheme with the resonances $\rho(770) + \rho(1450) + \rho(1700) + \rho(2100)$ and the PP, VP, and AP loops in the polarization operators is used. This is scheme 2:

Scheme 2. The data on the reactions $e^+e^- \to \pi^+\pi^-$ [7], $e^+e^- \to \omega\pi^0$ [13], and $e^+e^- \to \pi^+\pi^-\pi^+\pi^-$ [14] are fitted separately in the model, which takes into account the resonances $\rho(770) + \rho(1450) + \rho(1700) + \rho(2100)$ side by side while allowing for the PP, VP, and AP loops in the polarization operators.

The parameters found from the fitting scheme 2 are listed in Table I. Let us comment on each of the mentioned channels.

A. Fitting $e^+e^- \to \pi^+\pi^-$ data

When fitting the data on the reaction $e^+e^- \to \pi^+\pi^-$ at energies $\sqrt{s} \leq 1$ GeV in our previous publication [1–3], the fitting scheme 1 was used. There, the restriction to the PP loop was justifiable because of the rather low energies under consideration. Using the resonance parameters found from fitting the data in the time-like region, the pion form factor $F_\pi(s)$ in the space-like region $s < 0$ was calculated up to $-s = Q^2 = 0.2$ GeV^2 and compared with the NA7 data [9]. A comparison with the data [10–12] in the wider range up to $-s = Q^2 = 10$ GeV^2 was made in Ref. [3]. In the present work, we give the corresponding plot in Fig. 5 for the sake of completeness. The continuation to the space-like domain in the fitting scheme 2 is discussed below.

The cross section of the reaction $e^+e^- \to \pi^+\pi^-$ fitted in scheme 2 is shown in Fig. 6. As far as the $\rho(770)$ resonance parameters are concerned, one can observe that in comparison with the fit in scheme 1 [1–3], the bare mass of the resonance ρ_1 determined in scheme 2 in the sensitive channel $e^+e^- \to \pi^+\pi^-$ is typically lower. (Compare Table I here and Table I in, e.g., Ref. [1].) The same concerns the coupling constant g_{ρ_1} which

TABLE I. The resonance parameters found from fitting the data on the reactions $e^+e^- \to \pi^+\pi^-$ [7], $e^+e^- \to \pi^+\pi^-\pi^+\pi^-$ [14], and $e^+e^- \to \omega\pi^0$ [13], in the fitting scheme 2 (see text). The parameter $\mathrm{Re}\Pi'_{\omega\rho}$ is responsible for $\omega\rho$ mixing; see Ref. [1] for more details. The parameter g_{ρ_4} can be found from the sum rule $\frac{g_{\rho_1\pi\pi}}{g_{\rho_1}} + \frac{g_{\rho_2\pi\pi}}{g_{\rho_2}} + \frac{g_{\rho_3\pi\pi}}{g_{\rho_3}} + \frac{g_{\rho_4\pi\pi}}{g_{\rho_4}} = 1$, which provides the correct normalization $F_\pi(0) = 1$.

Parameter	$e^+e^- \to \pi^+\pi^-$	$e^+e^- \to \pi^+\pi^-\pi^+\pi^-$	$e^+e^- \to \omega\pi^0$
m_{ρ_1} [MeV]	765.6 ± 0.1	$\equiv 777$	$\equiv 777$
$g_{\rho_1\pi\pi}$	6.336 ± 0.004	5.78 ± 0.01	6.63 ± 0.03
g_{ρ_1}	4.662 ± 0.002	5.66 ± 0.02	4.80 ± 0.02
$g_{\rho_1 a_1\pi}$ [GeV^{-1}]	2.37 ± 0.05	0.26 ± 0.02	5.61 ± 0.08
m_ω [MeV]	782.02 ± 0.10	$\equiv 782.02$	$\equiv 782.02$
$\mathrm{Re}\Pi'_{\omega\rho}$ [GeV^2]	$(4.38 \pm 0.07) \times 10^{-3}$	—	—
m_{ρ_2} [MeV]	1507 ± 3	1122 ± 1	1412 ± 6
$g_{\rho_2\pi\pi}$	-6.01 ± 0.03	-5.45 ± 0.03	-5.72 ± 0.08
g_{ρ_2}	78 ± 2	8.74 ± 0.04	$21.6 \pm .4$
$g_{\rho_2\omega\pi}$ [GeV^{-1}]	6.66 ± 0.07	38.2 ± 0.2	32 ± 2
$g_{\rho_2 a_1\pi}$ [GeV^{-1}]	1.48 ± 0.11	5.61 ± 0.03	-1.37 ± 0.15
m_{ρ_3} [MeV]	1831 ± 4	1648 ± 1	1661 ± 5
$g_{\rho_3\pi\pi}$	-2.800 ± 0.008	3.681 ± 0.005	-0.90 ± 0.03
g_{ρ_3}	8.45 ± 0.05	4.302 ± 0.005	4.90 ± 0.04
$g_{\rho_3\omega\pi}$ [GeV^{-1}]	5.32 ± 0.02	0.98 ± 0.02	22.0 ± 0.3
$g_{\rho_3 a_1\pi}$ [GeV^{-1}]	0.41 ± 0.06	-1.692 ± 0.005	3.1 ± 0.1
m_{ρ_4} [MeV]	2154 ± 15	2390 ± 5	1969 ± 7
$g_{\rho_4\pi\pi}$	-1.78 ± 0.03	-4.5 ± 0.1	-3.11 ± 0.08
$g_{\rho_4\omega\pi}$ [GeV^{-1}]	8.65 ± 0.12	11.39 ± 0.05	8.19 ± 0.10
$g_{\rho_4 a_1\pi}$ [GeV^{-1}]	1.63 ± 0.05	1.004 ± 0.035	-0.91 ± 0.02
$m_{K_1(1270)}$ [MeV]	$\equiv 1270$	1265 ± 1	1230 ± 7
$m_{a_1(1260)}$ [MeV]	$\equiv 1230$	1132 ± 1	1268 ± 4
$\Gamma_{a_1(1260)}$ [MeV]	—	1028 ± 3	—
s_0 [GeV]^2	4.33 ± 0.03	0.00037 ± 0.00001	0.09 ± 0.03
$\chi^2/N_{\mathrm{d.o.f.}}$	335/316	400/59	43/20

parametrizes the leptonic decay width (1.3). The coupling constant $g_{\rho_1\pi\pi}$ in scheme 2 is greater than in scheme 1. The above distinction can be qualitatively explained by the effect of the renormalization of the coupling constants described in Ref. [1]. Indeed, as was shown in Ref. [1], the renormalization results in the substitutions

$$g_{\rho_1\pi\pi} \to Z_\rho^{-1/2} g_{\rho_1\pi\pi}, \qquad g_{\rho_1} \to Z_\rho^{1/2} g_{\rho_1}, \tag{4.1}$$

where

$$Z_\rho = 1 + \frac{d\,\mathrm{Re}\Pi_{\rho_1\rho_1}(s)}{ds}\bigg|_{s=m_{\rho_1}^2}. \tag{4.2}$$

Equation (4.1) means that the bare $g_{\rho_1\pi\pi}$ obtained from the fit is related to the "physical" one obtained from the visible peak, upon multiplying by $Z_\rho^{1/2}$, while the opposite is true for g_{ρ_1}. The contributions of the VP loop to $d\,\mathrm{Re}\Pi_{\rho_1\rho_1}/ds$ near $s = m_{\rho_1}^2$, as is observed from Fig. 1, are positive and exceed the negative contribution from the PP loop; see Fig. 7 in Ref. [1]. The same is true for the AP loop. As a result, one has $Z_\rho > 1$.

Although the energy behavior of the cross section up to $\sqrt{s} = 1.7$ GeV is described in the adopted model, including the dip near 1.5 GeV, one can see that the structure in the interval 2–2.5 GeV demands, in all appearance, additional ρ-like resonances and/or intermediate states in the loops. We tried to include the contribution of $K_1(1400)\bar{K}$ + c.c. states coupled solely to the resonance ρ_4, with the fitted coupling constant $g_{\rho_4 K_1(1400)K}$ and mass $m_{K_1(1400)}$. This slightly improves the agreement in the interval $1.75 < \sqrt{s} < 2$ GeV but occurs at the expense of adding two additional free parameters and does not result in reproducing the peak near $\sqrt{s} = 2.3$ GeV.

The continuation to the space-like region $s < 0$ with the resonance parameters obtained in the region $s > 4m_\pi^2$ in fitting scheme 2 with the VP and AP loops added results in unwanted behavior of $F_\pi(s)$; see Fig. 7. Specifically, the curve goes through experimental points [9] up to $s = -0.2$ GeV^2, but at larger values of $-s = Q^2$ one encounters infinities arising from the Landau poles due to the VP and AP loops. As was pointed out in Ref. [1], the Landau pole is present even in the case of the PP loop, but its position is at $\sqrt{Q^2} \approx 90$ GeV, that is, it is far from accessible momentum transfers. In the case of the VP and AP loops the Landau poles appear in the region accessible to existing experiments [10–12]

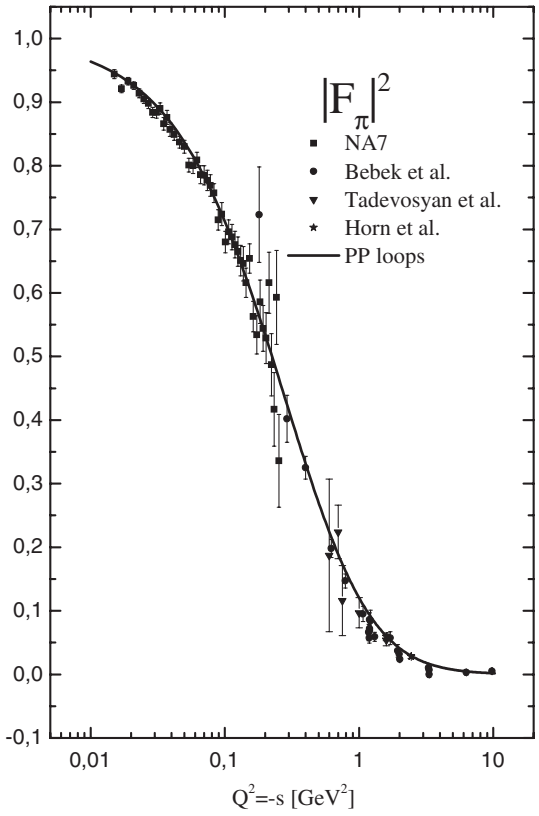

FIG. 5. The pion form factor squared in the space-like region $s < 0$ evaluated using the resonance parameters of Table I in Ref. [1] (the *BABAR* column) using fitting scheme 1 (see text). The experimental data are from NA7 [9], Bebek *et al.* [10], Horn *et al.* [11], and Tadevosyan *et al.* [12].

because of the large magnitude of the coupling constant $g_{\rho_1\omega\pi} = 13.2\ \mathrm{GeV}^{-1}$ [30].

An important feature of the new expression for the pion form factor obtained in Ref. [1] which was not mentioned there is that it does not require [3] the commonly accepted Blatt-Weisskopf centrifugal factor [31]

$$C_\pi(k) = \frac{1 + R_\pi^2 k_R^2}{1 + R_\pi^2 k^2}$$

in the expression for $\Gamma_{\rho\pi\pi}(s)$ [21]. Here k is the pion momentum at some arbitrary energy while k_R is its value at the resonance energy. The fact is that the usage of the R_π-dependent centrifugal barrier penetration factor in particle physics—for example, in the case of the $\rho(770)$ meson [21]—results in the overlooked problem. Indeed, the meaning of R_π is that this quantity is the characteristic of the potential (or the t-channel exchange in field theory) resulting in the phase δ_{bg} of the potential scattering in addition to the resonance phase [31]. For example, in case of the P-wave scattering in the potential

$$U(r) = G\delta(r - R_\pi),$$

where the resonance scattering is possible, the background phase is

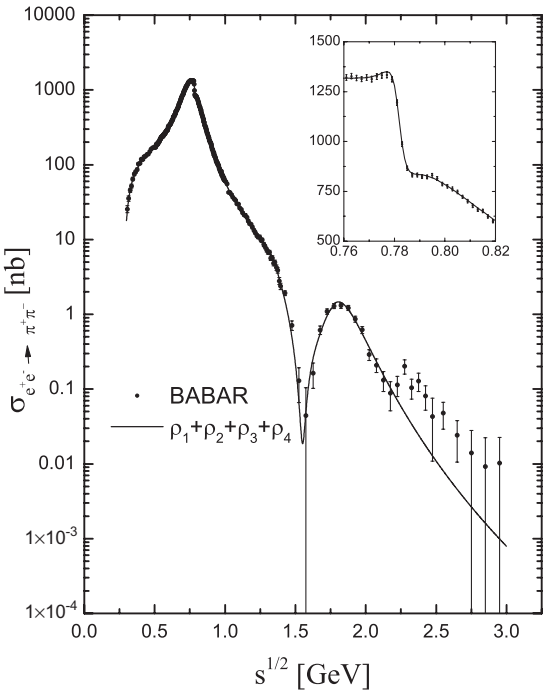

FIG. 6. The cross section of the reaction $e^+e^- \to \pi^+\pi^-$. The data are from Ref. [7] and the curve is drawn using the resonance parameters of scheme 2. The $\rho - \omega$ resonance region is shown in the insert.

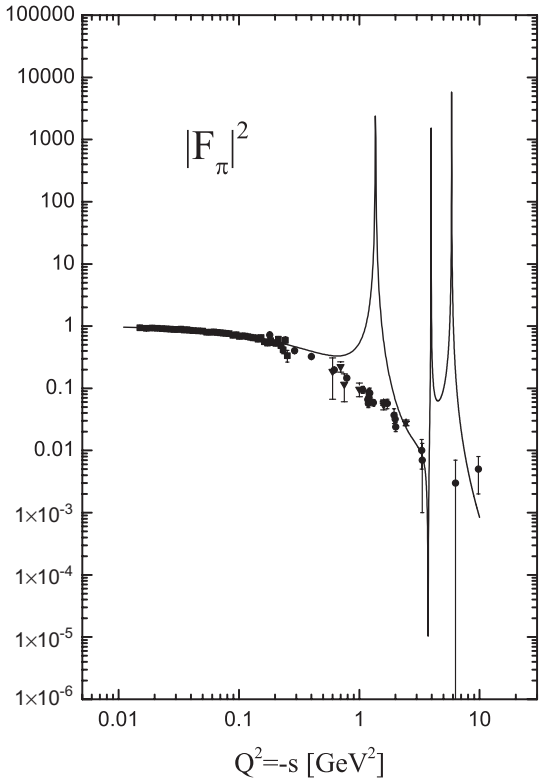

FIG. 7. The same as in Fig. 5, but with the resonance parameters obtained in fitting scheme 2 (see text).

$$\delta_{\rm bg} = -R_\pi k + \arctan(R_\pi k).$$

At the usual value of $R_\pi \sim 1$ fm, $\delta_{\rm bg}$ is not small. However, in the ρ-meson region, the background phase shift $\delta_{\rm bg}$ is negligible and the phase shift δ_1^1 is completely determined by the resonance; see Fig. 8 in Ref. [1]. Therefore, the descriptions of the hadronic resonance distributions which invoke the parameter R_π, have a dubious character.

B. Fitting $e^+e^- \to \pi^+\pi^-\pi^+\pi^-$ data

The dynamics of the reaction $e^+e^- \to \pi^+\pi^-\pi^+\pi^-$ at energies $\sqrt{s} < 1$ GeV is determined by the chiral-invariant mechanisms whose amplitudes are too cumbersome to include into the loop integrations for the purposes of fits. Hence we restrict ourselves to the energy range $1 < \sqrt{s} < 3$ GeV dominated by the $\rho(1450)$, $\rho(1450)$, ... s-channel production mechanism. The energy dependence of the $e^+e^- \to \pi^+\pi^-\pi^+\pi^-$ reaction cross section is shown in Fig. 8. One can see that at energies $\sqrt{s} > 1.75$ GeV the chosen scheme with three heavier rho-like resonances $\rho_{2,3,4}$ cannot reproduce the structures in the measured cross section such as the bizarre sharp turn in the energy behavior followed by fluctuations. As in the case of the reaction $e^+e^- \to \pi^+\pi^-$, the contributions of the AP loops $a_1(1260)\pi$ and $K_1(1270)\bar{K}$ + c.c. coupled to all ρ_i resonances ($i = 1, 2, 3, 4$) were invoked to explain the features above 1.75 GeV. The structures remain unexplained.

As is seen from Table I, the coupling constants g_{ρ_1} and $g_{\rho_1\pi\pi}$ of the $\rho(770)$ meson found from fitting this channel differ from those found from fitting the $\pi^+\pi^-$ one. Furthermore, the coupling constant $g_{\rho_1 a_1 \pi}$ found from fitting the channel $e^+e^- \to \pi^+\pi^-\pi^+\pi^-$ is suppressed in comparison with the naive chiral-symmetry estimate $g_{a_1\to\rho_1\pi} \sim 1/2f_\pi \sim 5\,\text{GeV}^{-1}$ [32], where $f_\pi = 92.4$ MeV is the pion decay constant. We believe that this difference is an artifact of the oversimplified $a_1\pi$ model and the price that comes with the possibility of using the analytical calculation of the VP and AP loops to simulate the contributions of the multiparticle meson states in polarization operators [33]. In the meantime, the coupling constants $g_{\rho_1 a_1 \pi} \approx 2.4$ and $5.6\,\text{GeV}^{-1}$ found from fitting the $e^+e^- \to \pi^+\pi^-$ and $e^+e^- \to \omega\pi^0$ channels, respectively, look sensible. For comparison, the estimates of $g_{\rho_1 a_1 \pi}$ in the model adopted in the present work are $\sim 6\,\text{GeV}^{-1}$ and $\sim 4\,\text{GeV}^{-1}$, as extracted from $\Gamma_{a_1} \approx 0.6$ GeV and 0.3 GeV [21], respectively. Note also that $\Gamma_{a_1\to\rho\pi\to 3\pi} \sim 1$ GeV when evaluated in the generalized hidden local symmetry chiral model for $m_{a_1} \approx 1.2$ GeV [32]. The width of the visible peak in Fig. 8 is about 0.44 GeV, which should be compared with $\Gamma_{\rho_3}(\sqrt{s} = m_{\rho_3}) = 0.45$ GeV evaluated with the $\pi^+\pi^-\pi^+\pi^-$ column of Table I.

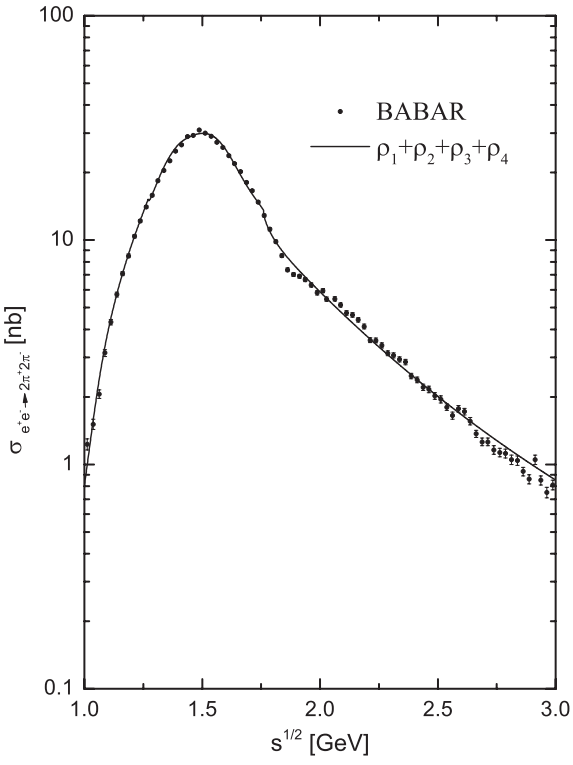

FIG. 8. The cross section of the reaction $e^+e^- \to \pi^+\pi^-\pi^+\pi^-$. The data are from Ref. [14] and the curve is drawn using the resonance parameters of scheme 2.

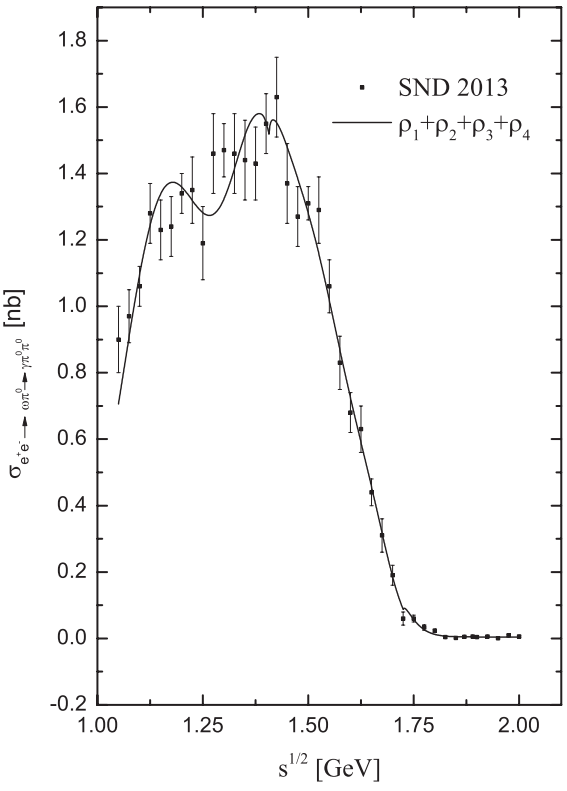

FIG. 9. The cross section of the reaction $e^+e^- \to \omega\pi^0 \to \pi^0\pi^0\gamma$. The data are from SND13 [13] and curve is drawn using the resonance parameters of scheme 2.

C. Fitting $e^+e^- \to \omega\pi^0$ data

Quite recently, new data on the reaction $e^+e^- \to \omega\pi^0$ in the decay mode $\omega \to \pi^0\gamma$ were published by the SND collaboration [13]. They are analyzed with fitting scheme 2. The resulting curve calculated with the parameters cited in Table I is shown in Fig. 9.

V. CONCLUSION

The main purpose of the present work is to describe the pion electromagnetic form factor $F_\pi(s)$ up to the J/ψ energy range, using the expression obtained in Ref. [1]. This expression, when restricted to the PP loops in polarization operators, permits a good description of the data of SND, CMD-2, KLOE, and *BABAR* on $\pi^+\pi^-$ production in e^+e^- annihilation at $\sqrt{s} < 1$ GeV, describes the scattering kinematical domain up to $-s = Q^2 = 10$ GeV^2, and does not contradict the data on the $\pi\pi$ scattering phase δ^1_1. The goal of extending the description to energies up to 3 GeV in the time-like domain was reached by the inclusion of the VP and AP loops in addition to the PP ones. These loops contain the couplings of the ρ-like resonances with the VP and AP states and generate, in turn, the final states $\omega\pi^0$ and $\pi^+\pi^-\pi^+\pi^-$ in e^+e^- annihilation. Therefore, consistency demands the treatment of these final states as well. As is shown in the present work, the energy behavior of the cross sections of the reactions $e^+e^- \to \omega\pi^0$ and $e^+e^- \to \pi^+\pi^-\pi^+\pi^-$ obtained in the adopted simplified model does not contradict the data. The statistically poor description of the cross section of the reaction $e^+e^- \to \pi^+\pi^-\pi^+\pi^-$ is, probably, an artifact of the oversimplified model for its amplitude, which ignores both the requirements of the chiral symmetry at lower energies and a complicated intermediate state at higher energies. The proper treatment of the reaction $e^+e^- \to \pi^+\pi^-\pi^+\pi^-$ is beyond the scope of the present work. Nevertheless, we included this poor description for the consistency of the presentation.

One should not wonder at the fact that the masses of heavier ρ-like resonances quoted in Table I differ from the values quoted in Ref. [21]. In fact, the values in Ref. [21] are only educated guesses, and the masses of heavier ρ-like resonances quoted by the Particle Data Group fall into wide intervals; for instance, $m_{\rho_2} = 1265$–1580 MeV and $m_{\rho_3} = 1430$–1850 MeV [21]. Furthermore, the quoted values are usually obtained from fitting the data with the help of the simplest parametrization such as the sum of the Breit-Wigner amplitudes. In the meantime it is known that the residues of the simple pole contributions do not necessarily reveal the true nature of the resonances involved in the process [34–36] when the mixings and dynamical effects like the final-state interaction become essential.

The real problem is that the continuation to the space-like domain of the expression for $F_\pi(s)$ with the contributions of the VP and AP loops meets the difficulty of encountering the Landau poles. By all appearances, this is the consequence of the chosen parametrization of the vertex form factor which restricts the growth of the partial widths as the energy increases in a modest way. A stronger suppression could effectively suppress the couplings of rho-like resonances with the VP and AP states and, in turn, push the Landau zeros to higher space-like momentum transfers. This is the topic of a separate study.

ACKNOWLEDGMENTS

We are grateful to M. N. Achasov for numerous discussions which stimulated the present work. This work is supported in part by the Russian Foundation for Basic Research Grant no. 13-02-00039 and the Interdisciplinary project No 102 of the Siberian Division of the Russian Academy of Sciences.

[1] N. N. Achasov and A. A. Kozhevnikov, Phys. Rev. D **83**, 113005 (2011); **85**, 019901 (2012).
[2] N. N. Achasov and A. A. Kozhevnikov, Nucl. Phys. B, Proc. Suppl. **225–227**, 10 (2012).
[3] N. N. Achasov and A. A. Kozhevnikov, Pis'ma v ZhETF **96**, 627 (2012) [JETP Lett. **96**, 559 (2013)].
[4] M. N. Achasov *et al.*, Zh. Eksp. Teor. Fiz. **101**, 1201 (2005) [J. Exp. Theor. Phys. **101**, 1053 (2005)].
[5] R. R. Akhmetshin *et al.* (CMD-2 Collaboration), Phys. Lett. B **648**, 28 (2007).
[6] F. Ambrosino *et al.* (KLOE Collaboration), Phys. Lett. B **700**, 102 (2011).
[7] B. Aubert *et al.* (The *BABAR* Collaboration), Phys. Rev. Lett. **103**, 231801 (2009).
[8] N. N. Achasov and A. A. Kozhevnikov, Phys. Rev. D **55**, 2663 (1997).
[9] S. R. Amendolia *et al.*, Nucl. Phys. **B277**, 168 (1986).
[10] C. J. Bebek *et al.*, Phys. Rev. D **17**, 1693 (1978).
[11] T. Horn *et al.*, Phys. Rev. Lett. **97**, 192001 (2006).
[12] V. Tadevosyan *et al.*, Phys. Rev. C **75**, 055205 (2007).
[13] M. N. Achasov *et al.*, Phys. Rev. D **88**, 054013 (2013).
[14] J. P. Lees *et al.* (The *BABAR* Collaboration), Phys. Rev. D **85**, 112009 (2012).
[15] M. Benayoun, P. David, L. DelBuono, and F. Jegerlehner, Eur. Phys. J. C **73**, 2453 (2013).
[16] M. Benayoun, P. David, L. DelBuono, and F. Jegerlehner, Eur. Phys. J. C **72**, 1848 (2012).
[17] M. Benayoun and H. B. O'Connell, Eur. Phys. J. C **22**, 503 (2001).
[18] H. Czyz, A. Grzelinska, and J. H. Kuhn, Phys. Rev. D **81**, 094014 (2010).
[19] C. Hanhart, Phys. Lett. B **715**, 170 (2012).

[20] We use this opportunity to correct the misprint in the expression for $\Pi_1^{(PP)}$ in Refs. [2,3] where the braces were omitted when typesetting.
[21] J. Beringer *et al.* (Particle Data Group), Phys. Rev. D **86**, 010001 (2012).
[22] N. N. Achasov and A. A. Kozhevnikov, Phys. Rev. D **62**, 056011 (2000).
[23] N. N. Achasov and A. A. Kozhevnikov, Zh. Eksp. Teor. Fiz. **91**, 499 (2000) [J. Exp. Theor. Phys. **91**, 433 (2000)].
[24] N. N. Achasov and A. A. Kozhevnikov, Pis'ma v ZhETF **88**, 3 (2008) [JETP Lett. **88**, 1 (2008)].
[25] N. N. Achasov and A. A. Kozhevnikov, Eur. Phys. J. A **38**, 61 (2008).
[26] H. Czyz, J. H. Kuhn, and A. Wapienik, Phys. Rev. D **77**, 114005 (2008).
[27] H. Czyz and J. H. Kuhn, Eur. Phys. J. C **18**, 497 (2001).
[28] G. Ecker, J. Gasser, A. Pich, and E. De Rafael, Nucl. Phys. **B321**, 311 (1989).
[29] R. R. Akhmetshin *et al.* (CMD-2 Collaboration), Phys. Lett. B **466**, 392 (1999).
[30] The coupling constant $g_{\rho_1\omega\pi}$ is extracted from the partial width of the decay $\omega(782) \to \pi^+\pi^-\pi^0$.
[31] J. M. Blatt and V. F. Weisskopf, *Theoretical Nuclear Physics,* (Wiley, New York, 1952).
[32] N. N. Achasov and A. A. Kozhevnikov, Phys. Rev. D **71**, 034015 (2005).
[33] Of course, more sophisticated models which take into account other possible mechanisms of the four-pion production in e^+e^- annihilation and tau lepton decay (see for example Refs. [26–28]) result in a better agreement with the data. Nevertheless, we give here the results of fitting the $e^+e^- \to \pi^+\pi^-\pi^+\pi^-$ data in the scheme with the simplest quasi-two-body mechanism because it is this mechanism which is used here in modelling the pion form factor. We believe that it is appropriate to investigate the consequences of the model used for the form factor (which is the main goal of the present study) for other processes. A proper description of the four-pion production cross section is a separate problem.
[34] N. N. Achasov and G. N. Shestakov, Phys. Rev. Lett. **99**, 072001 (2007).
[35] N. N. Achasov and A. V. Kiselev, Phys. Rev. D **83**, 054008 (2011).
[36] N. N. Achasov and A. V. Kiselev, Phys. Rev. D **85**, 094016 (2012).